Nano Energy 88 (2021) 106303

Contents lists available at ScienceDirect

Nano Energy

journal homepage: www.elsevier.com/locate/nanoen

Full paper

Performance enhanced triboelectric nanogenerator by taking advantage of water in humid environments

Dong Liu [a,1], Jinmei Liu [a,1], Maosen Yang [a], Nuanyang Cui [a], Haoyu Wang [a], Long Gu [a,*], Longfei Wang [c,d,**], Yong Qin [b,*]

[a] School of Advanced Materials and Nanotechnology, Xidian University, Xi'an 710071, China
[b] Institute of Nanoscience and Nanotechnology, School of Materials and Energy, Lanzhou University, Gansu 730000, China
[c] School of Material Science and Engineering, Georgia Institute of Technology, Atlanta, Georgia 30332, United States
[d] Beijing Institute of Nanoenergy and Nanosystems, Chinese Academy of Sciences, Beijing 101400, China

ARTICLE INFO

Keywords:
Triboelectric nanogenerator
Humidity resisting
Energy harvesting
PVA/LiCl film
Self-powered system

ABSTRACT

Improving the performance of triboelectric nanogenerator (TENG) in environment with high humidity is critical for their applications in blue energy, humidity sensing, implantable nanodevice etc. Here, we report a kind of humidity-resisting TENG (HR-TENG) by using polyvinyl alcohol/lithium chloride (PVA/LiCl) as the triboelectric layer, the output of which is much enhanced (~5 times) with the increase of relative humidity (RH, from 20% to 99%). Abundant hydroxyl groups in PVA can fix water molecules to form more tribo-positive surface polarity, and LiCl can regulate the water absorption ability of PVA/LiCl film. The combined effect brings in numbers of wrinkle microstructure on its surface and synchronously decreases its modulus, enabling more efficient contact. Charge density of the HR-TENGs are higher than 115 μC/m^2 in a wide range of RH (from 60% to 99%), especially, reaches a maximum value of 244 μC/m^2 in 90% RH, which is much larger than the highest value 110 μC/m^2 among reported HR-TENGs (RH>50%). Moreover, the PVA/LiCl based TENGs can be acted as power source in high RH (93%) condition and respiratory monitoring sensor for human physiological monitoring. These results provide an efficient way for TENG with high output in high humidity environments.

1. Introduction

To satisfy the increasing demand of green and sustainable power supplies for widely applied intelligent electronic devices [1–3], energy harvesting technologies based on electromagnetic induction, piezoelectric effect [4–6], pyroelectric effect [7,8] and triboelectric effect [9–12] have been developed rapidly in recent years. Triboelectric nanogenerator (TENG), as one of the most promising energy harvesting technologies, has been extensively exploited to convert various kinds of mechanical energy from ambient environment into useful electrical energy. Benefitting from the advantages of low-cost, variable structure, easy fabrication, high energy conversion efficiency as well as favorable biological compatibility [13–15], TENG exhibits great capability of being a sustainable power source in most of application circumstances [16–18]. However, the diversity and variability of the application scenarios further require TENG to be highly adaptable to the working environment, especially in some harsh environments, such as high humidity conditions. Moisture in atmosphere can easily absorb on the friction layer's surface of TENG and form a layer of free water, which will accelerate the transmission and dissipation process of the triboelectric charges on friction surface [19]. As a result, the output and stability of TENG will be severely degraded. Therefore, how to achieve high output performance of the TENG in high humidity environment is still a big issue.

To address this problem, several humidity-resisting TENGs (HR-TENG) have been proposed by utilizing encapsulated package or superhydrophobic triboelectric materials [20–25]. For example, Xu et al. [26] and Mule et al. [27] encapsulated TENGs into a closed drying space which could effectively protect TENGs from the negative influence of moisture. By using this method, stable output performance was successfully realized in relative humidity (RH) range of 40–80%. In addition, Li et al. [28] and Lee et al. [29] introduced micro/nano structure or

* Corresponding authors.
** Corresponding author at: School of Material Science and Engineering, Georgia Institute of Technology, Atlanta, Georgia 30332, United States.
E-mail addresses: lgu@xidian.edu.cn (L. Gu), lfwang12@binn.cas.cn (L. Wang), qinyong@lzu.edu.cn (Y. Qin).
[1] Authors with equal contribution.

https://doi.org/10.1016/j.nanoen.2021.106303
Received 21 May 2021; Received in revised form 24 June 2021; Accepted 28 June 2021
Available online 1 July 2021

hydrophobic groups on the frictional layers to lower the surface energy and hence achieve superhydrophobic surfaces, which could prevent the absorption of moisture and further mitigate the output degradation in high humidity conditions. Moreover, considering that the encapsulation and hydrophobization process are cumbersome, complicated and inappropriate for large-scale application of TENGs, Chang et al. [30,31] designed TENGs with water bridge theory, in which charge transfer increases the surface charge density and hence enhances the output of TENGs in humid environments. Subsequently, Wang et al. [32] also developed a starch film based TENG with an enhanced output performance in humidity ambience, the output current density and charge density of which increase from 0.42 μA/cm^2, 8 μC/cm^2 to 1.04 μA/cm^2, 27.8 μC/cm^2 respectively when the RH increases from 15% to 95%. These studies have gradually increased the performance of TENG in humid environments, but the output is still relatively low, especially in high RH, and needs to be further improved. If the environment humidity can be used to largely increase the output performance of TENG in humid environments with a wide range of RH, it will be great valuable.

In this work, we developed a kind of HR-TENG based on PVA/LiCl composite film which can take advantage of water in humid environments to realize a high output in wide range of RH (from 60% to 99%). Benefitting from the enhanced tribo-positive property, roughened surface, and soft contact causing by decreased modulus in humid environments, the output performance of PVA/LiCl based HR-TENGs is largely improved in high humidity conditions. Through controlling the water absorption ability of PVA/LiCl film by adding different mass ratio of LiCl, the output charge density of HR-TENG is always higher than 115 μC/m^2 in high RH (from 60% to 99%). Especially, the maximum output voltage and current of the HR-TENG reach 670 V and 37 μA in RH 90%, the corresponding charge density is 244 μC/m^2, which is 2.21 times larger than the highest value of 110 μC/m^2 among reported HR-TENGs (RH>50%). In addition, The HR-TENG used as a power source in high RH (93%) and as humidity sensor for human physiological monitoring have been successfully developed.

2. Experimental section

2.1. Preparation of PVA and PVA/LiCl films

Firstly, 4.8 g PVA powder (Aladdin Reagents Co., Ltd, degree of alcoholysis: 99.0–99.4 mol%, viscosity: 12.0–16.0 mPa s) was added into 40 mL distilled water with stirring and 90 ℃ water bath until it was completely dissolved. Secondly, different amounts of LiCl (Shanghai Jufeng Chemical Technology Co., Ltd) were added into PVA solution after it cooled down to room temperature, forming PVA/LiCl solution with mass ratio of 12:1, 18:1, 24:1, 30:1 respectively. Thirdly, PVA/LiCl solution was spinning coated on an aluminum electrode attached on acrylic sheet. The spinning coating parameter was 500 rpm for 5 s and 2000 rpm for 10 s. Finally, the prepared films were dried on a hot plate at 80 °C for 5 min, and then PVA and PVA/LiCl films with thickness about 15 μm could be obtained.

2.2. Preparation of PVDF and nylon films

2 g PVDF powder (Aladdin Reagents Co., Ltd) was added into 8 g DMF (Sinopharm Chemical Reagents Co., Ltd.) with stirring and 80 °C water bath until it was completely dissolved. The obtained PVDF solution was spin-coated on a silicon wafer (2000 rpm, 10 s), and then dried on a hot table at 110 °C for 2 min. PVDF film with thickness of 20 μm could be easily peeled off from Si wafer. As for nylon, 2 g nylon was added into 4.8 g formic acid (Sinopharm Chemical Reagents Co. Ltd) and 3.2 g dichloromethane (Tianjin Fuyu Fine Chemicals Co. Ltd) into a conical flask with stirring for 1 h until it was completely dissolved. With the same fabrication process of PVDF film, nylon film with thickness of 30 μm was obtained.

2.3. Fabrication of micro structured PTFE film via plasma etching

Precut PTFE film was firstly put into the ICP cavity, and then oxygen atmosphere (2 Pa) and input power of 100 W were adopted to etch the surface of PTFE for 30 min

2.4. Fabrication of PVA/LiCl based TENGs

The spinning-coated PVA, PVA/LiCl or nylon film with size of 25 mm×25 mm on aluminum foil electrode were used as positive friction layer. The precut PVDF (25 mm×25 mm) and PTFE (30 mm×30 mm) films were attached on a clean flat acrylic plate (40 mm×40 mm×1 mm) with aluminum electrode, which were used as the negative friction part. PVA, PVA/LiCl and nylon film was paired with PVDF or PTFE film to construct TENGs with contact-separation mode respectively. All TENGs were placed in a humidity chamber with RH 20% before measurement.

2.5. Fabrication of respiratory airflow driven TENG

An acrylic tube with inner dimensions of 50 mm×30 mm×15 mm was made by a laser cutter. Aluminum foils with spinning coated PVA/LiCl film were attached on the top and bottom surface of the small chamber via double sided tape as the electrode and positive friction layers. One end of the plasma etched PTFE (50 mm×25 mm×0.05 mm) was fixed onto the middle plane of the acrylic tube as the negative friction layer. Keeping the other end of PTFE film free-standing so that it could fluctuate up and down when respiratory airflow came through.

2.6. Characterization and measurement

The mechanical tensile test was carried out using ESM301/Mark-10 system. The gauge size of the sample was about 10 mm×5 mm×0.8 mm. For tensile tests, the speed was fixed at 10 mm/min. The SEM images were taken by Apreo HiVac (FEI, USA), and optical microscope images were taken by Leica DM2700M RL/TL. For the electrical measurement of TENGs, a linear motor (Linmot E1100) was used to provide the periodical mechanical stimulus. Low noise preamplifiers (Stanford, SR570) and Keithley electrometer 6514 were used to measure the output current and voltage. PCI-6259 (National Instruments) was used for data collection. A software platform based on Labview was used to realize real-time data acquisition and analysis. As for the testing environment control, a sealed cuboid chamber with two inlets and one outlet was utilized to accurately control the humidity. An air inlet and an outlet for dry air are on the left side of chamber. A flow meter is used to control the air inlet and outlet respectively. The right side of the chamber is the other air inlet which is used to control the humid air flow. The three flowmeters can be adjusted depending on the indication of the hygrometer in the chamber so that the required relative humidity can be accurately achieved.

3. Results and discussion

Generally, the output of TENGs decreases as the RH increases due to the aggravated dissipation of triboelectric charges resulted by free water film adsorbed on the friction layers. For example, as shown in Fig. S1, with the RH increasing from 20% to 99%, the output voltage and current of a TENG based on commonly used PVDF and nylon are gradually reduced by 84% and 79%, respectively. To conquer this reducing trend of TENG's output, the HR-TENG composed of PVA and PVDF is designed. Its fabrication process and working mechanism are schematically shown in Fig. 1**a**. The output of PVA/PVDF based TENG exhibits a completely different trend with the increasing of RH. As shown in Fig. 1**b**, the output voltage firstly decreases from 12.1 V to 4.8 V with the RH increasing from 20% to 60%, and then sharply increases to 42.8 V, which is 3.5 times of the initial value when the RH continuously increased to 99%. The output current also presents the same tendency,

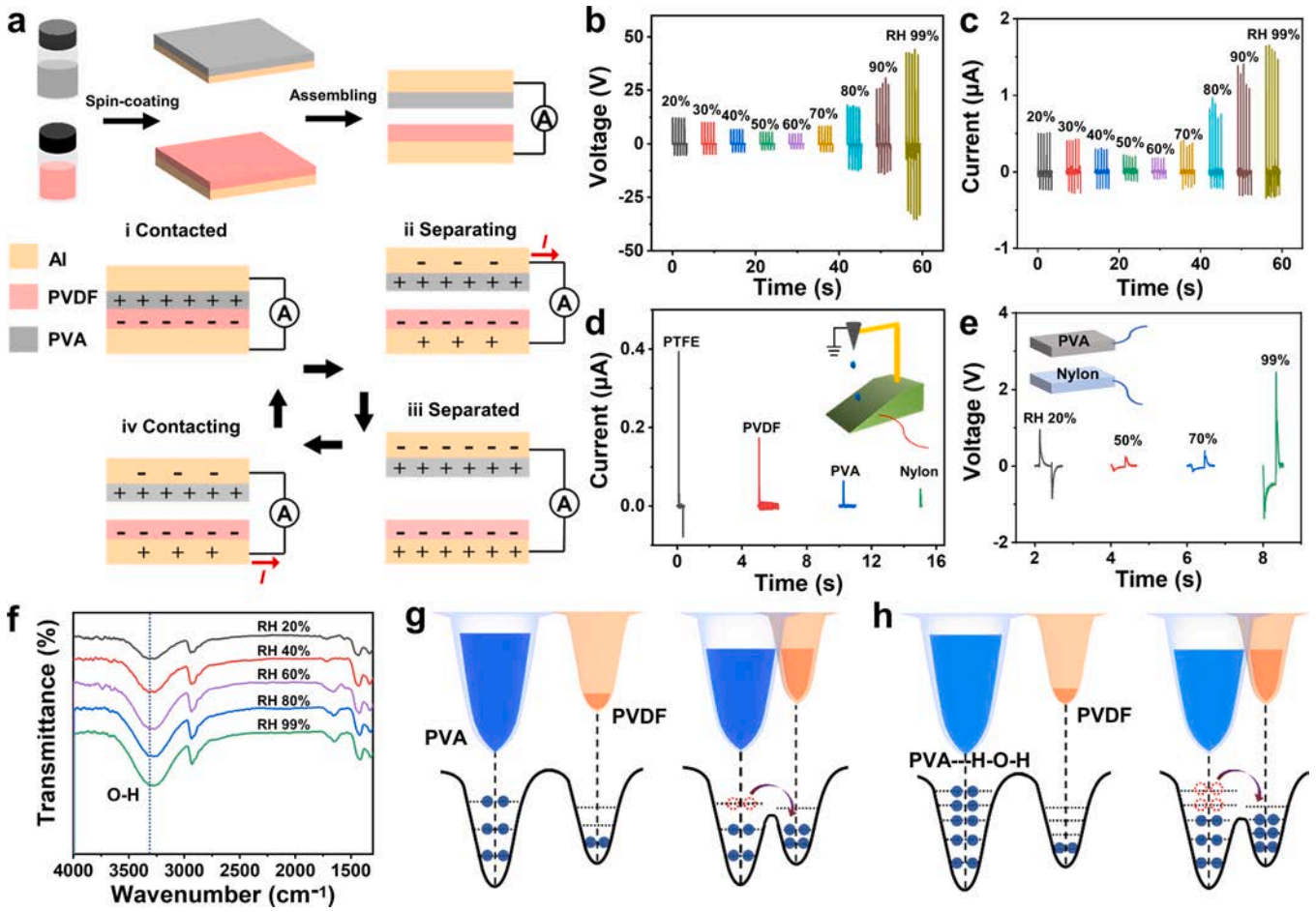

Fig. 1. The mechanism of PVA film to enhance the output of HR-TENG. a, The fabrication process and working mechanism of the HR-TENG composed of PVA and PVDF. **b, c,** The output voltage and current of the HR-TENG in different RH conditions. **d,** The output current of single electrode TENG which composed of PTFE, PVDF, PVA and nylon with water, respectively. **e,** The output voltage of TENG based on nylon/PVA in different RH conditions. **f,** 100 °C-variable temperature infrared spectra of PVA film at different RH conditions. **g, h,** Schematic diagrams of electron transfer mechanism of PVA and PVA with hydrogen bonding water molecules (PVA—H-O-H) rubbing with PVDF.

which firstly decreases from 0.5 μA to 0.17 μA and then increases to 1.64 μA (Fig. 1**c**). The output performances of PVDF/nylon-based TENG and PVDF/PVA-based HR-TENG imply that PVA has the capability to enhance the output performance of TENG in high humidity environments.

To deeply understand the mechanism of output performance enhancement of PVA based HR-TENG in high RH conditions, a reasonable hypothesis that the water molecules involve in the friction process is proposed. To verify this assumption, we carry out a series of comparative experiments based on TENGs with single-electrode working mode. Water droplet is used as the positive triboelectric material, PTFE, PVDF, dry PVA and nylon are adopted as the negative triboelectric layer, respectively. Schematic diagram of the setup and output of the four kinds of TENGs are shown in Fig. 1**d**. It can be found that all output current peaks of the four TENGs are firstly positive and then negative, which indicates that dry PVA and nylon show tribo-negative polarity compared with water, which are same with PTFE and PVDF. In addition, a TENG based on the dry PVA and nylon films are fabricated, and its output voltages at RH 20%, 50%, 70%, and 99% are measured and shown in Fig. 1**e**. As the RH increases from 20% to 50%, the voltage signal of the TENG is reversed. With the further increase of RH to 99%, the output voltage increases significantly. These results indicate that the relative polarity of PVA and nylon could be completely reversed by water molecules, and gradually become larger. The interaction of PVA and water molecules is further studied by the 100 °C-variable temperature infrared spectrum of PVA in different RH conditions. As the formation of hydrogen bonds can average the surrounding electron cloud of oxygen atom, the absorption peak intensity and location of hydroxyl group will increase and move to the low wave direction respectively, as shown in Fig. 1**f**. As a contrast, no obvious distinction is observed from the spectrums of nylon in different RH conditions (Fig. S2), which indicates that no bonding effect existed between water molecules and nylon. These results demonstrate that PVA can absorb water molecules to enhance its tribo-positive property via hydrogen bonding in the humid environment. The triboelectric charges transfer mechanisms of PVA and PVA with hydrogen bonding water (PVA—H-O-H) rubbing with PVDF are schematically shown in Fig. 1**g** and **h**, respectively. With the RH increasing, more absorbed water molecules on PVA participate in the friction process, of which the increasing triboelectric charges are counteracted by the negative effect of water on PVDF at the beginning and then substantially increase the output of HR-TENG in high RH conditions. As a result, there is competition between the enhanced positive triboelectric property of PVA and the dissipative effect of PVDF by water. Thus, the output of PVA based HR-TENG shows a special variation tendency of first decrease and then increase with the increasing of RH, and eventually realized a much higher output in high RH conditions.

The maximum output (42.8 V, 0.17 μA) of PVA based HR-TENG is still relative small and that can only be realized in very high RH (99%) condition. In order to achieve higher output in wide range of RH con-

ditions, the hygroscopic property of PVA is enhanced by introducing LiCl with strong polar ionic bonds. Thus, more water can be absorbed into the gaps of PVA molecular chains in addition to the surface bonded water molecules, which can significantly change the surface structure and the mechanical property of PVA/LiCl film and hence results in a further increase in the output of HR-TENG. As PVA/LiCl sol solution is spin-coated on a rigid substrate and then dry to form a dense film, there will be initial tension on the surface of the film. When water molecules are absorbed into the film, this tension will be released and results in local swelling of PVA/LiCl film. Owing to the water content gradient along the thickness of PVA/LiCl film, its surface area tends to increase, while the bottom layer restricted by the rigid substrate below is almost unchanged. As a result, anisotropic osmotic pressure along the thickness direction of PVA/LiCl is generated. When the osmotic pressure is greater than the critical value, the net compressive stress forces the outer surface to bend, resulting in the formation of surface wrinkle microstructure, as shown in Fig. 2**a**. According to the linear expansion theory, the wavelength of the fold pattern λ_0 depends on the thickness of the film and the mechanical properties of the film and substrate [33,34]:

$$\lambda_0 = 2\pi t\left(\frac{\overline{E}_f}{3\overline{E}_s}\right)^{1/3} \quad A_0 = t\left(\frac{\varepsilon_0}{\varepsilon_c} - 1\right)^{1/2} \tag{1}$$

$$\varepsilon_c = -\frac{1}{4}\left(\frac{3\overline{E}_s}{\overline{E}_f}\right)^{2/3} \tag{2}$$

Thereinto, $\overline{E}_f$ and $\overline{E}_s$ represent the plane strain modulus of PVA/LiCl film and rigid substrate respectively. The wavelength of wrinkle λ_0 and the amplitude A_0 are related to the thickness (t) of PVA/LiCl film. ε_0 represents the applied strain and ε_c is given as the critical strain which is the minimum strain required for wrinkling.

To systematically investigate the influence of LiCl on the formation of surface wrinkle microstructure, the morphology of PVA/LiCl films (mass ratio of 18:1) and pure PVA film in different RH conditions (20%, 40%, 60%, 80% and 99%) are characterized by optical microscope. For the pure PVA film (Fig. 2**b**), its surface is flat and smooth when RH is lower than 40%, while a few circle-like structures appear at RH 60%. These circle-like structures eventually turn into large wrinkle with size

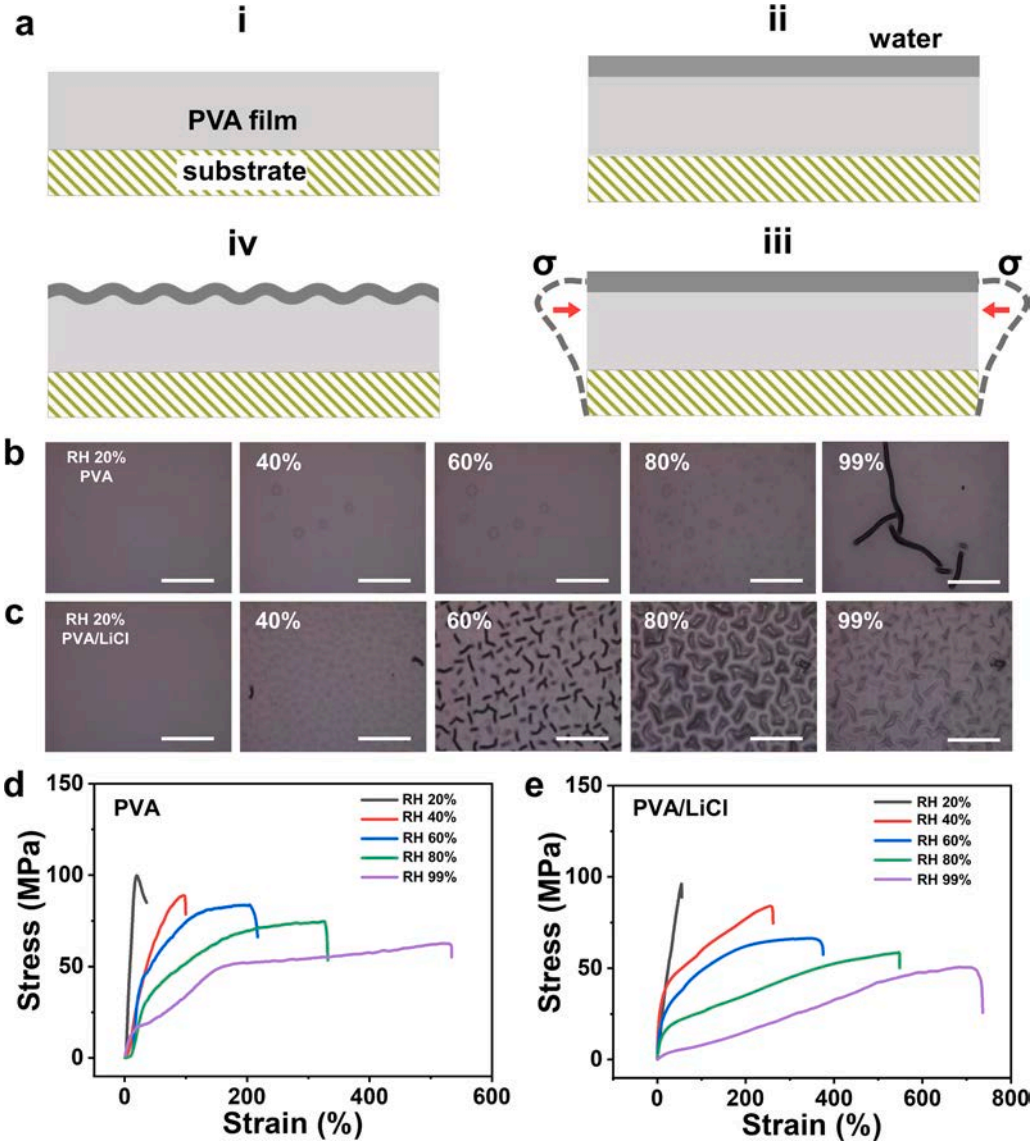

Fig. 2. The generation mechanism and characterization of wrinkle microstructure on PVA/LiCl film. **a,** Schematic diagram of swelling induced wrinkling process. **b, c,** Optical morphology images of PVA and PVA/LiCl films in different RH conditions. All scale bars represent 50 μm. **d, e**, The stress-strain curves of PVA and PVA/LiCl films in different RH conditions.

larger than 500 μm when RH further increases to 99%. For the PVA/LiCl film (18:1) (Fig. 2**c**), lots of circle-like structures appear at RH 40%, then turn into wrinkle microstructure at RH 60%, and finally become fuzzy when the RH increases to 99% due to absorbing too much water. The water-induced wrinkle microstructures on PVA/LiCl film are characterized by atomic force microscope (AFM), as shown in Fig. S3. The height of the wrinkle microstructure gradually increases with the increasing of RH. Moreover, as the hygroscopic property of PVA/LiCl film is closely associated to the content of LiCl (Fig. S4), the surface microstructure of PVA/LiCl films (30:1, 24:1, 12:1) are investigated (Fig. S5). It can be found that PVA/LiCl film with more LiCl has smaller size and higher density of wrinkle microstructure. As these PVA/LiCl films are of the same thickness and spin-coated on the same material based substrate (Al foil), the wrinkle microstructure on the PVA/LiCl films is mainly resulted by their different mechanical property according to the formulas (1) and (2).

The stress-strain curve of the pure PVA and PVA/LiCl films (mass ratio of 18:1) in different RH (from 20% to 99%) conditions are shown in Fig. 2**d** and **e**. The results show that the modulus of two films significantly decreases with the increase of RH. Compared with pure PVA film, the modulus of PVA/LiCl film decreases much faster due to its stronger water absorption ability enhanced by LiCl. The much lower modulus of PVA/LiCl film in humid conditions leads to the formation of small size and high density wrinkle microstructure on PVA/LiCl film. The resulted roughened surface can effectively enhance the output performance of TENG. In addition, the low modulus of PVA/LiCl film also enables a soft and complete contact between the two triboelectric layers and results in more effective friction, which can further improve the output of PVA/LiCl based HR-TENG (Fig. 3**a**).

To demonstrate the combined effect of PVA and LiCl, we fabricate HR-TENGs (with size of 2.5 cm×2.5 cm) composed of PVA/LiCl (18:1) and PVDF and characterize their output performance. As shown in Fig. 3**b** and **c**, as RH increases from 20% to 30%, the output voltage and current dropped slightly, and then sharply increased as RH further increases from 30% to 70%, which show a similar tendency to PVA based HR-TENG but with a different turning point. When RH is higher than 70%, the outputs of PVA/LiCl based HR-TENG begin to decrease. The overall variation tendency is a balanced result of the positive effect of hydrogen bonding water (enhanced positive triboelectric polarity), the surface wrinkle microstructure, decreased modulus (enables a soft and complete contact) and the negative effect of charge dissipation resulted by free water. It should be noted that the maximum output voltage and current are as high as 490 V and 18 μA, which are 11.5 and 10.5 times of the maximum values of PVA based HR-TENG, respectively, whereas the RH corresponding to the maximum output is reduced from 99% to 70%. The decrease in output of HR-TENG in high RH (from 70% to 99%) is mainly due to the dominated charge dissipation effect of water. The charge density of HR-TENGs based on PVA/LiCl films with different mass ratio of LiCl (30:1, 24:1, 18:1,12:1) and pure PVA film are calculated from their output current (Fig. 3**d**). It can be found that the

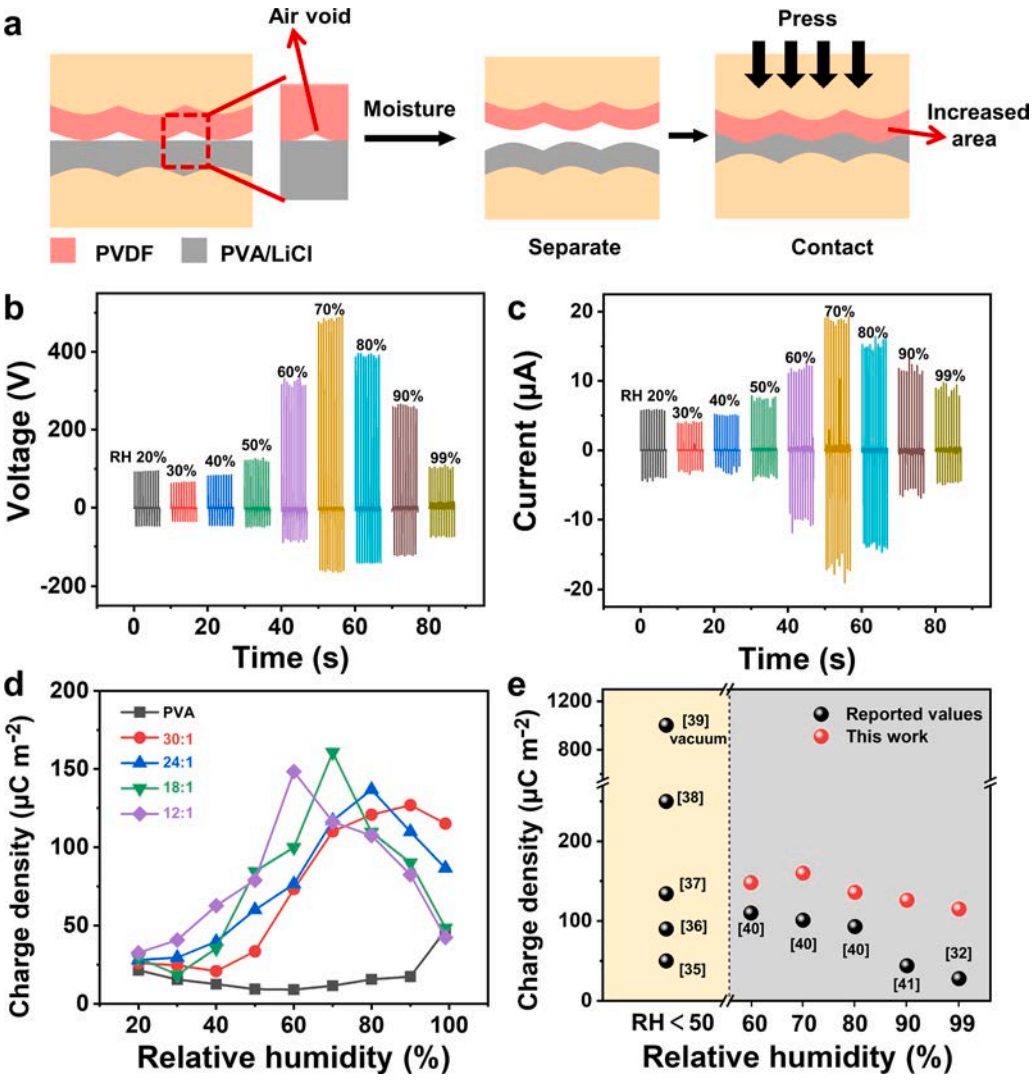

Fig. 3. The output performance of PVA/LiCl based HR-TENGs. **a,** Low modulus of PVA/LiCl film in RH conditions enables a soft and complete contact between the two triboelectric layers and results in more effective friction. **b, c,** The output voltage and current of PVA/LiCl (mass ratio of 18:1) based HR-TENG at different RH conditions. **d,** The charge density of PVA and PVA/LiCl (mass ratios of 30:1, 24:1, 18:1 and 12:1) based HR-TENGs at different RH conditions. **e,** Maximum charge density of PVA/LiCl based TENGs in high RH conditions (60%, 70%, 80%, 90% and 99%), and some selected representative TENGs.

maximum charge density of all PVA/LiCl films based HR-TENGs are higher than 115 μC/m^2, and the RH corresponding to the maximum value is gradually moved to a lower RH with the increasing amount of LiCl, which indicates that high output performance of HR-TENG in wide range of high RH conditions can be achieved through controlling the amount of LiCl. Moreover, without considering the structure enhanced TENGs such as charge-pumping and self-charging TENGs etc., a comparison just from perspective of triboelectric materials among TENGs is shown in Fig. 3**e**. The maximum charge density in all reported HR-TENGs in high RH conditions (RH from 60% to 99%) are counted here. It can be found that the charge density of our HR-TENG in RH from 60% to 99% are all the highest, which are even comparable to the values of reported TENGs in low RH (<50%) conditions [35–41].

The output performance of HR-TENG could also be influenced by external impact force and contact frequency. Here, we use the PVA/LiCl (mass ratio of 18:1) based HR-TENG in RH 70% to investigate the influence of external impact force and contact frequency on its output performance. Driven by different forces with a frequency of 2 Hz, the output voltage, current density and charge density of PVA/LiCl based TENG are measured (Fig. 4**a** and **b**). As the applied force increases from 2 N to 20 N, the output voltage increases steadily from 442 V to 562 V, and the corresponding output current density and charge density present similar trends increasing from 17.4 mA/m^2 to 33.5 mA/m^2, and from 91.1 μC/m^2 to 190.6 μC/m^2, respectively. This phenomenon can be explained by the increased effective contact area causing by the larger driven force. The correlation between output voltage, current density, charge density and contact frequency is shown in Fig. 4**c** and **d**. Under a driven force of 20 N, when the contact frequency increases from 0.5 Hz to 3 Hz, the output voltage raises from 345 V to 572 V, the corresponding output current density and the charge density increases from 23.8 mA/m^2 to 35.5 mA/m^2, and from 120.4 μC/m^2 to 182.5 μC/m^2, respectively. A longevity test of the HR-TENG is likewise carried out at RH 70%, and the output voltage keeps stable in more than 10,000 working cycles without any degradation (Fig. 4**e**), which shows its excellent durability and stability. Moreover, the HR-TENG exhibits sensitive response to the variation of RH, as shown in Fig. 4**f**. With the

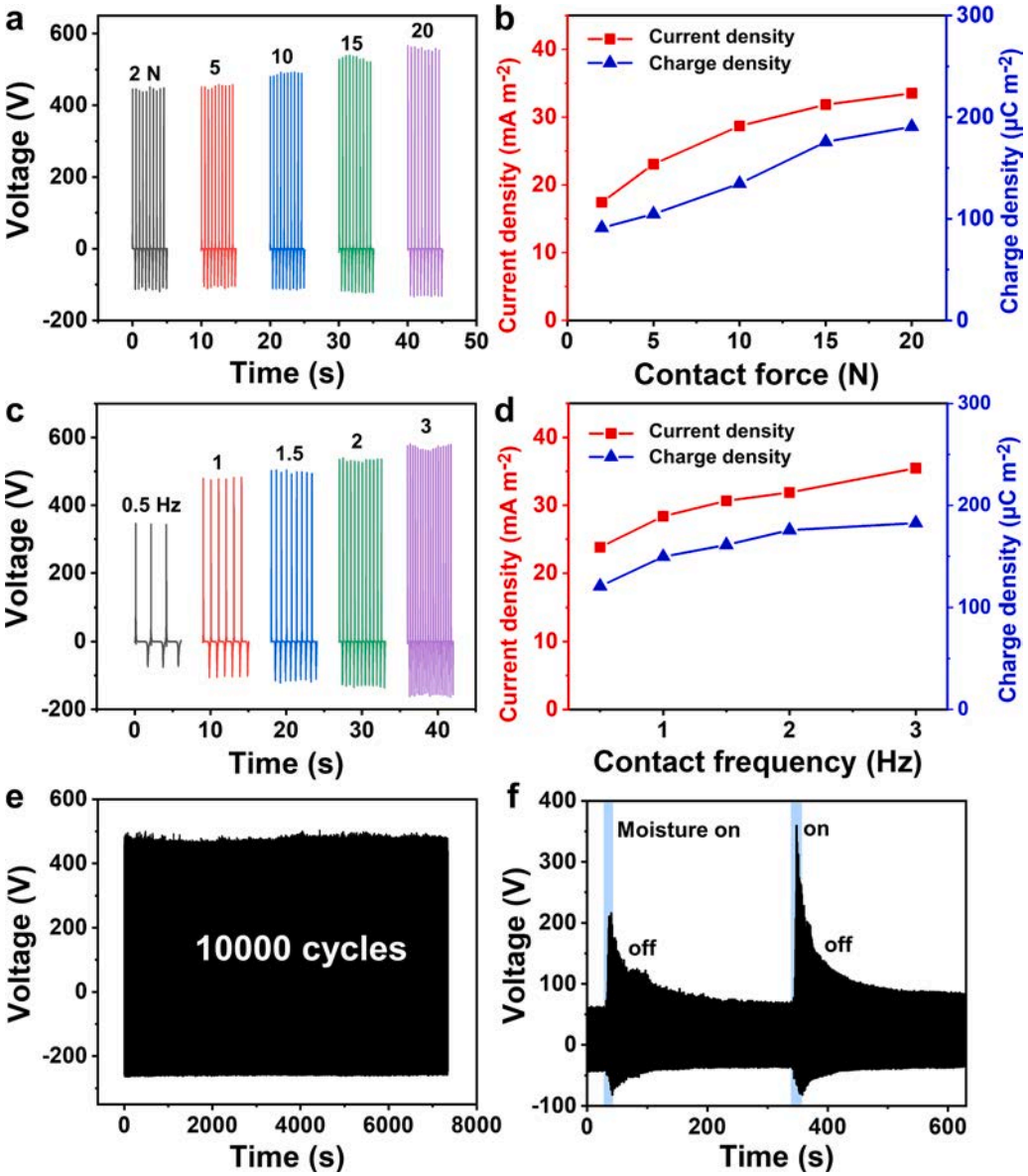

Fig. 4. The influence of external impact force and contact frequency on the output performance of HR-TENG. **a, b,** The output voltage, current density, and charge density of the HR-TENGs under different driving forces. **c, d,** The output voltage, current density and charge density of the HR-TENGs under different contact frequency. **e,** Long cycle stability test of HR-TENG. **f,** The response of HR-TENG to the variation of relative humidity in environment.

moisture on, the output voltage of HR-TENG increases rapidly, and when the moisture turns off, the output voltage drops slowly due to the slow desorption process of water molecules on the surface of PVA/LiCl film. When the water source approaches to the HR-TENG again, the PVA/LiCl film can still reabsorb water molecules resulting in a rabidly upgrade in the output voltage. These results demonstrate the excellent property of HR-TENG in response to the fluctuation of humidity.

To further enhance the output performance, more tribonegative polytetrafluoroethylene (PTFE) is used to pair with PVA/LiCl film (30:1) for assembling a HR-TENG (with size of 3 cm×3 cm). Meanwhile, plasma etching technology is adopted to introduce micro structure on the surface of PTFE (Fig. S6). The output voltage and current are up to 664 V and 37 μA at RH 90% (Fig. 5**a** and **b**), and the corresponding charge density reaches 244 $\mu C/m^2$ (Fig. S7) which is 2.21 times of the highest values among reported HR-TENG. The excellent output performance enables the HR-TENG suitable to be a sustainable micro power source in high RH conditions. As shown in Fig. 5**c** and Supplementary Movie S1, PVA/LiCl/PTFE based HR-TENG is placed in a custom-made airtight box and electrically connected with 160 green LEDs. When the RH increases to 93%, these LEDs can be instantaneously lighted up, which indicates that the HR-TENG can be utilized to construct a self-powered warning system in some factories where humidity conditions are strictly controlled. In order to power some high energy consumption electronic devices in high RH conditions, the output power of the HR-TENG needs to be stored in a capacitor. A bridge rectifier circuit connected with HR-TENG is utilized to convert the AC output into DC signals that can directly charge a capacitor, as shown in Fig. 5**d**. A 47 μF capacitor is charged to 2.5 V in about 110 s at RH 92% (Fig. 5**e**), and the stored electric energy can drive a commercial hygrometer (Fig. 5**f**).

Moreover, the PVA/LiCl based HR-TENG can be used as a more efficient and self-powered respiratory monitoring sensor for real-time human physiological monitoring by taking advantage of moisture in breathing air. A respiratory airflow driven HR-TENG composed of PVA/LiCl and PTFE is designed and fabricated, and the schematic diagram of working mechanism is shown in Fig. S8. To analyze the exhalation process, electrical signals of three different breathing states, including the state of strenuous exercise, the relaxed state and the deep breathing are recorded (Fig. 5**g–i**). Different respiration states produce distinctive electrical output characteristics. After strenuous exercise, the respiratory frequency is short and rapid, and 12 characteristic peaks of output current appear within 20 s (Fig. 5**g**). The width of the peak group is 0.9 s and the peak value of output current reaches 1.45 μA. When people stayed in the calm or relaxed state, the respiration rate is slow, and only four characteristic peaks of output current appear within 20 s (Fig. 5**h**). The width of the peak group is 1.25 s and the peak value of output current is 1.2 μA, which are all lower than that of the state of strenuous exercise. The breathing time of deep breathing is the longest, and hence the corresponding characteristic peak of output current is widest (3.8 s)

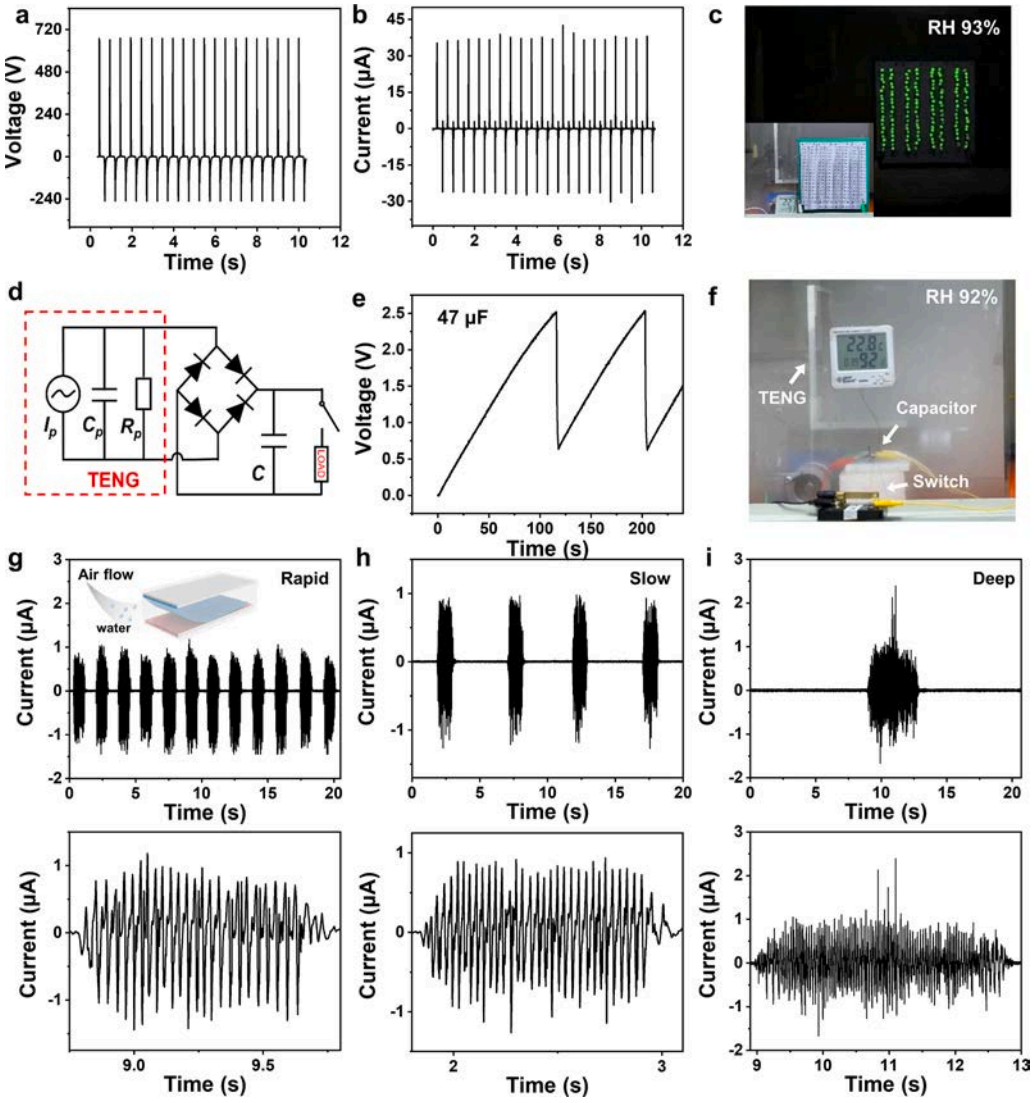

Fig. 5. Applications of PVA/LiCl based HR-TENG in high RH conditions. **a, b,** The output voltage and current of the HR-TENG composed of PTFE and PVA/LiCl at RH 90%. **c,** HR-TENG used as a micro power source to light up 160 green LEDs at RH 92%. **d,** Diagram of the energy storage circuit. **e,** Charging and discharging curve for a 47 μF capacitor by using HR-TENG. **f,** HR-TENG acted as a micro power source to power a hygrometer at RH 92%.**g–i,** HR-TENG used as an efficient and self-powered respiratory monitoring sensor for real time monitoring of human respiratory.

(Fig. 5**i**). The enlarged views of the output in different breathing states show that all signals slowly raise at the beginning, then remain relatively stable in the middle, and finally drop gradually, which are commendably matched the breathing behavior of a human body. These results demonstrate the great potential of the HR-TENG for constructing self-powered human monitoring systems.

4. Conclusions

In summary, we developed a kind of humidity-resisting TENG with high performance by using PVA/LiCl composite film, which could take advantage of water in humid environments to enhance its output performance in wide range of RH (60−99%). Benefitting from the special triboelectric property of PVA/LiCl composite in humid conditions: (1) abundant hydroxyl groups in PVA can fix water molecules through hydrogen bond and form more tribo-positive surface polarity; (2) LiCl as an strong hygroscopic salt can precisely regulate the water absorption ability of PVA/LiCl film; (3) the local swelling induced by water absorption results in a large number of wrinkle structures which can effectively roughen the surface of PVA/LiCl film; (4) the decreased modulus of PVA/LiCl enables soft and more efficient contact between the friction layers. Owing to the combined effect of PVA and LiCl, the output charge density of PVA/LiCl based TENGs are always higher than 115 μC/m^2 in wide range of high RH conditions (from 60% to 99%). Especially, the maximum output voltage and current of our TENG at RH 90% reach 670 V and 37 μA, and the corresponding charge density is up to 244 μC/m^2. Furthermore, the TENGs can be applied as power source in high humid environments and self-powered human monitoring device. This work provides a feasible and effective way to design and fabricate high performance TENG in high RH conditions.

Associate contents

Supporting Information comprising Supplementary Figure 1: the output voltage and current of TENG based on PVDF and nylon under different RH conditions.; Supplementary Figure 2: infrared spectra of nylon film at different RH from 20% to 99%; Supplementary Figure 3: the wrinkle microstructure of PVA/LiCl film (18:1) under different humidity characterized by atomic force microscopy; Supplementary Figure 4: water absorption of PVA and PVA/LiCl films at RH 90% within 1 h; Supplementary Figure 5: the surface morphology of PVA/LiCl films with different mass ratios (30:1, 24:1, 12:1) at RH 20%, 40%, 60%, 80% and 99%.; Supplementary Figure 6: the SEM images of initial PTFE and PTFE with micro structure; Supplementary Figure 7: enlarge view of HR-TENG's output current shown in Fig. 5b; Supplementary Figure 8: working mechanism of the respiratory airflow driven HR-TENG for real-time breath monitoring; Supplementary Movie 1: 160 green LEDs is instantaneously lighted up by HR-TENG in humid environment (RH 93%).

CRediT authorship contribution statement

Dong Liu: Investigation. **Jinmei Liu:** Investigation. **Maosen Yang:** Investigation. **Nuanyang Cui:** Visualization. **Haoyu Wang:** Methodology. **Long Gu:** Conceptualization, Writing - original draft. **Longfei Wang:** Writing - original draft, Writing - review & editing. **Yong Qin:** Conceptualization, Writing - review & editing, Supervision.

Declaration of Competing Interest

The authors declare that they have no known competing financial interests or personal relationships that could have appeared to influence the work reported in this paper.

Acknowledgements

This research was supported by the National Natural Science Foundation of China, China, No. 81801847, the Natural Science Basic Research Plan in Shaanxi Province of China, China, No. 2021JQ-200, the Fundamental Research Funds for the Central Universities, China, No. QTZX2183, the Joint fund of Equipment pre-Research and Ministry of Education, China, NO. 6141A02022518, and the National Program for Support of Top-notch Young Professionals, China.

Appendix A. Supporting information

Supplementary data associated with this article can be found in the online version at doi:10.1016/j.nanoen.2021.106303.

References

[1] D.Y. Park, D.J. Joe, D.H. Kim, H. Park, J.H. Han, C.K. Jeong, H. Park, B. Jeong, K. J. Lee, Self-powered real-time arterial pulse monitoring using ultrathin epidermal piezoelectric sensor, Adv. Mater. 29 (2017) 1702308–1702316.
[2] Z.L. Wang, Triboelectric nanogenerators as new energy technology and self-powered sensors - principles, problems and perspectives, Faraday Discuss. 176 (2014) 447–458.
[3] C. Xia, J. Yang, W. Ning, Z.L. Wang, Triboelectric nanogenerators driven self-powered electrochemical processes for energy and environmental science, Adv. Energy Mater. 6 (2016), 1600665.
[4] R.S. Yang, Y. Qin, L.M. Dai, Z.L. Wang, Power generation with laterally packaged piezoelectric fine wires, Nat. Nanotechnol. 4 (2009) 34–39.
[5] C. Chang, V.H. Tran, J.B. Wang, Y.K. Fuh, L.W. Lin, Direct-write piezoelectric polymeric nanogenerator with high energy conversion efficiency, Nano Lett. 10 (2010) 726–731.
[6] X.D. Wang, Piezoelectric nanogenerators-harvesting ambient mechanical energy at the nanometer scale, Nano Energy 1 (2012) 13–24.
[7] L.C. Rome, L. Flynn, E.M. Goldman, T.D. Yoo, Generating electricity while walking with loads, Science 309 (2005) 1725–1728.
[8] Y. Yang, W.X. Guo, K.C. Pradel, G. Zhu, Y.S. Zhou, Y. Zhang, Y.F. Hu, L. Lin, Z. L. Wang, Pyroelectric nanogenerators for harvesting thermoelectric energy, Nano Lett. 12 (2012) 2833–2838.
[9] F.R. Fan, Z.Q. Tian, Z.L. Wang, Flexible triboelectric generator, Nano Energy 1 (2012) 328–334.
[10] Z.L. Wang, Triboelectric nanogenerators as new energy technology for self-powered systems and as active mechanical and chemical sensors, ACS Nano 7 (2013) 9533–9557.
[11] S. Kim, M.K. Gupta, K.Y. Lee, A. Sohn, S.W. Kim, Transparent flexible graphene triboelectric nanogenerators, Adv. Mater. 26 (2014) 3918–3925.
[12] Z.L. Wang, J. Chen, L. Lin, Progress in triboelectric nanogenerators as a new energy technology and self-powered sensors, Energy Environ. Sci. 8 (2015) 2250–2282.
[13] G. Zhu, B. Peng, J. Chen, Q. Jing, Z.L. Wang, Triboelectric nanogenerators as a new energy technology: from fundamentals, devices, to applications, Nano Energy 14 (2015) 126–138.
[14] Q. Zhang, Z. Zhang, Q. Liang, F. Gao, F. Yi, M. Ma, Q. Liao, Z. Kang, Green hybrid power system based on triboelectric nanogenerator for wearable/portable electronics, Nano Energy 55 (2018) 151–163.
[15] X. Peng, K. Dong, C. Ye, Y. Jiang, Z.L. Wang, A breathable, biodegradable, antibacterial, and self-powered electronic skin based on all-nanofiber triboelectric nanogenerators, Sci. Adv. 26 (2020) eaba9624.
[16] N.Y. Cui, L. Gu, J.M. Liu, S. Bai, J. Qiu, J. Fu, X. Kou, H. Liu, Y. Qin, Z.L. Wang, High performance sound driven triboelectric nanogenerator for harvesting noise energy, Nano Energy 15 (2015) 321–328.
[17] X.F. Wang, S.M. Niu, Y.J. Yin, F. Yi, Z. You, Z.L. Wang, Triboelectric nanogenerator based on fully enclosed rolling spherical structure for harvesting low-frequency water wave energy, Adv. Energy Mater. 5 (2015) 1501467–1501475.
[18] Q. Zheng, H. Zhang, B.J. Shi, X. Xue, Z. Liu, Y. Ma, Y. Zou, X.X. Wang, Z. An, W. Tang, W. Zhang, Fan Yang, Y. Liu, X.L. Lang, Z.Y. Xu, Z. Li, Z.L. Wang, In vivo self-powered wireless cardiac monitoring via implantable triboelectric nanogenerator, ACS Nano 10 (2016) 6510–6518.
[19] V. Nguyen, R. Yang, Effect of humidity and pressure on the triboelectric nanogenerator, Nano Energy 2 (2013) 604–608.
[20] D. Jang, Y. Kim, T.Y. Kim, K. Koh, U. Jeong, J.H. Cho, Force-assembled triboelectric nanogenerator with high-humidity-resistant electricity generation using hierarchical surface morphology, Nano Energy 20 (2016) 283–293.
[21] K.N. Kim, J. Chun, W.K. Jin, K.Y. Lee, J.U. Park, S.W. Kim, Z.L. Wang, J.M. Baik, Highly stretchable 2D fabrics for wearable triboelectric nanogenerator under harsh environments, ACS Nano 9 (2015) 6394–6400.
[22] Y.T. Jao, P.K. Yang, C.M. Chiu, A textile-based triboelectric nanogenerator with humidity-resistant output characteristic and its applications in self-powered healthcare sensors, Nano Energy 50 (2018) 513–520.
[23] M.Y. Ma, Q.L. Liao, G.J. Zhang, Z. Zhang, Self-recovering triboelectric nanogenerator as active multifunctional sensors, Adv. Funct. Mater. 25 (2015) 6489–6494.

[24] S. Yan, J. Lu, W. Song, R. Xiao, Flexible triboelectric nanogenerator based on cost-effective thermoplastic polymeric nanofiber membranes for body-motion energy harvesting with high humidity-resistance, Nano Energy 48 (2018) 248–255.
[25] Q. Zhou, K. Lee, K.N. Kim, High humidity- and contamination-resistant triboelectric nanogenerator with superhydrophobic interface, Nano Energy 50 (2019) 513–520.
[26] L. Xu, Y.K. Pang, C. Zhang, T. Jiang, X.Y. Chen, J.J. Luo, W. Tang, X. Cao, Z. L. Wang, Integrated triboelectric nanogenerator array based on air-driven membrane structures for water wave energy harvesting, Nano Energy 31 (2017) 351–358.
[27] A.R. Mule, B. Dudem, S.A. Graham, J.S. Yu, Humidity sustained wearable pouch-type triboelectric nanogenerator for harvesting mechanical energy from human activities, Adv. Funct. Mater. 29 (2019) 1807779–1807789.
[28] Z.L. Li, J.L. Shen, I. Abdalla, J.Y. Yu, B. Ding, Nanofibrous membrane constructed wearable triboelectric nanogenerator for high performance biomechanical energy harvesting, Nano Energy 36 (2017) 341–348.
[29] K.Y. Lee, J.S. Chun, J.H. Lee, K.N. Kim, N.R. Kang, J.Y. Kim, M.H. Kim, K.S. Shin, M.K. Gupta, J.M. Baik, S.W. Kim, Hydrophobic sponge structure-based triboelectric nanogenerator, Adv. Mater. 26 (2014) 5037–5042.
[30] T.H. Chang, Y.W. Peng, C.H. Chen, T.W. Chang, J.M. Wu, Z. H. Lin, Protein-based contact electrification and its uses for mechanical energy harvesting and humidity detecting, Nano Energy 21 (2016) 238–246.
[31] J. Shen, Z. Li, J. Yu, B. Ding, Humidity-resisting triboelectric nanogenerator for high performance biomechanical energy harvesting, Nano Energy 40 (2017) 282–288.
[32] N.N. Wang, Y.B. Zheng, Y.G. Feng, F. Zhou, D.A. Wang, Biofilm material based triboelectric nanogenerator with high output performance in 95% humidity environment, Nano Energy 77 (2020) 105088–105127.
[33] Y. Shu, K. Khare, P. Lin, Harnessing surface wrinkle patterns in soft matter, Adv. Funct. Mater. 20 (2010) 2550–2564.
[34] S. Zeng, L. Rui, S.G. Freire, E.Y. Huang, A.T. Smith, C. Hu, Z.C. Bian, G.A. Zheng, D. Y. Zhang, L.Y. Sun, Moisture-responsive wrinkling surfaces with tunable dynamics, Adv. Mater. 29 (2017), 1700828.
[35] J. Wang, Z. Wen, Y.L. Zi, P.F. Zhou, J. Lin, H.Y. Guo, Y.L. Xu, Z.L. Wang, All-plastic-materials based self-charging power system composed of triboelectric nanogenerators and supercapacitors, Adv. Funct. Mater. 26 (2016) 1070–1076.
[36] J. Wang, Z. Wen, Y.L. Zi, L. Lin, C.S. Wu, H.Y. Guo, Y. Xi, Y.L. Xu, Z.L. Wang, Self-powered electrochemical synthesis of polypyrrole from the pulsed output of a triboelectric nanogenerator as a sustainable energy system, Adv. Funct. Mater. 26 (2016) 3542–3548.
[37] S.M. Niu, J. Wang, Z. Wen, W. Tang, Z.L. Wang, Influence of chemical disorder on energy dissipation and defect evolution in concentrated solid solution alloys, Nat. Commun. 6 (2015) 8736.
[38] J. Wang, S. Li, F. Yi, Y. Zi, J. Lin, X.F. Wang, Y.L. Xu, Z.L. Wang, Sustainably powering wearable electronics solely by biomechanical energy, Nat. Commun. 7 (2016) 12744.
[39] J. Wang, C. Wu, Y. Dai, Z.H. Zhao, A. Wang, T.J. Zhang, Z.L. Wang, Achieving ultrahigh triboelectric charge density for efficient energy harvesting, Nat. Commun. 8 (2017) 88.
[40] F. Ejehi, R. Mohammadpour, E. Asadian, Graphene oxide papers in nanogenerators for self-powered humidity sensing by finger tapping, Sci. Rep. 10 (2020) 7312–7322.
[41] S. Yan, J.W. Lu, W. Song, R. Xiao, Flexible triboelectric nanogenerator based on cost-effective thermoplastic polymeric nanofiber membranes for body-motion energy harvesting with high humidity-resistance, Nano Energy 48 (2018) 248–255.

Dong Liu received his B.S. from the School of Chemistry and Chemical Engineering, Beijing Institute of Technology in 2018. He is now a graduate student at the School of Advanced Materials and Nanotechnology, Xidian University. His research interest focuses on the self-powered sensors based on triboelectric nanogenerators.

Jinmei Liu received her B.S and Ph.D. from the School of Physical Science and Technology of Lanzhou University in 2011 and 2016, respectively. She is currently a lecturer in School of Advanced Materials and Nanotechnology, Xidian University, China. Her research focuses on the design and synthesis of new materials for energy harvesting devices, flexible self-powered system. She has abundant experiences on synthesizing inorganic oxide nanowire arrays and nanofibers, and fabricating flexible functional nanodevices.

Maosen Yang received his M.S. from Shandong Normal University in 2018. He is now a Ph.D. student at the School of Advanced Materials and Nanotechnology, Xidian University. His research interest focuses on surface-enhanced raman spectroscopy, perovskite quantum dots, and self-powered sensors.

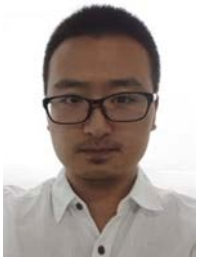

Nuanyang Cui received his Ph.D. in Material Physics and Chemistry from Lanzhou University, China in 2015. He currently is an associate professor in School of Advanced Materials and Nanotechnology, Xidian University. His current research focuses mainly on the dynamic behavior of the triboelectric charges in the triboelectric nanogenerator (TENG) and the enhancement mechanism of TENG.

Haoyu Wang is an undergraduate student in School of Advance Materials and Nanotechnology at Xidian University. His major is Materials Science and Engineering. His research interests are triboelectric nanogenerators and flexible electronic devices.

Long Gu received his B.S and Ph.D. from the School of Physical Science and Technology of Lanzhou University in 2010 and 2016, respectively. He is currently a lecturer in School of Advanced Materials and Nanotechnology, Xidian University, China. From 2020 to now, he worked as a postdoctoral fellow in Professor Xudong Wang's group at University of Wisconsin-Madison. His current research focuses on piezoelectric and triboelectric nanogenerator, functional nanodevices, and self-powered systems.

Longfei Wang received his Ph.D. in Nanoscience and Technology from Beijing Institute of Nanoenergy and Nanosystems, Chinese Academy of Sciences. From 2018–2021, he worked as a postdoctoral fellow in Professor Zhong Lin Wang's group at Georgia Institute of Technology. Now he is a professor in Beijing Institute of Nanoenergy and Nanosystems, Chinese Academic of Sciences. His current research focuses on the piezotronics, piezo-phototronics and functional nanodevice.

Yong Qin received his B.S. (1999) in Material Physics and Ph. D. (2004) in Material Physics and Chemistry from Lanzhou University. From 2007–2009, he worked as a visiting scholar and Postdoc in Professor Zhong Lin Wang's group at Georgia Institute of Technology. Currently, he is a professor at the Institute of Nanoscience and Nanotechnology, Lanzhou University, where he holds a Cheung Kong Chair Professorship. His research interests include nanoenergy technology, functional nanodevice and self-powered nanosystem. Details can be found at: http://www.yqin.lzu.edu.cn.